Semihard QCD and high-energy pp and $\bar{p}p$ scattering

Loyal Durand and Hong Pi
Department of Physics, University of Wisconsin-Madison, Madison, Wisconsin 53706
(Received 14 November 1988)

We present the results of an analysis of high-energy pp and $\bar{p}p$ scattering based on a model in which the energy dependence of very-high-energy processes is driven by semihard scatterings of quarks and gluons in the nucleons. We show in particular that parton-parton scattering processes at small x drive not only the observed increases in total, elastic-, and inelastic-scattering cross sections and the forward slope parameter, but also, through analyticity, a rapid increase in the ratio of the real to the imaginary part of the forward elastic-scattering amplitude. We also give a careful definition of the inclusive jet cross section and present results on $\sigma_{\rm jet}$, average jet multiplicities, and jet-multiplicity fluctuations at high energies.

I. INTRODUCTION

Semihard parton interactions appear to play an important role in high-energy hadronic scattering. For example, the onset of rapid growth in the nucleon-nucleon cross section can be associated at least qualitatively with the predicted increase with energy in the number of small, semihard QCD jets produced in a nucleon-nucleon collision[1,2] as seen in the UA1 "minijet" analysis.[3,4] Several models have been constructed which incorporate semihard parton-parton interactions in the treatment of high-energy nucleon-nucleon scattering.[1,2,5–10] The models differ in various respects, for example, whether or not they respect the constraints imposed by unitarity,[11] and in their treatment of QCD and "soft" processes, but have the common feature that the growth in the pp or $\bar{p}p$ cross section is associated with the rapid increase in the parton (mainly gluon) distribution functions at small values of the fraction x of the momentum of a nucleon carried by the parton. This feature seems to be essential for understanding the behavior of the nucleon-nucleon cross section at very high energies.[12]

We have reported elsewhere[6] on our predictions for the energy dependence of the pp and $\bar{p}p$ cross sections obtained from the QCD parton model using a diffraction-scattering formulation of the problem, and on predictions for the jet cross section, jet multiplicities, and fluctuations at very high energies.[7] We have since extended our calculations to include the expected real parts of forward-scattering amplitudes, and the slope parameters and cross-section differences for pp and $\bar{p}p$ scattering. In this paper, we summarize this work with emphasis on the new results. We show in particular that parton-parton scattering processes at small x drive not only the observed increase in total, inelastic, and elastic scattering cross sections, but also, through analyticity, a rapid increase in the ratio $\rho=\mathrm{Re}f(0)/\mathrm{Im}f(0)$ of the real to the imaginary parts of the forward elastic-scattering amplitude.

The remainder of the paper is organized as follows. In Sec. II, we summarize the basic theoretical input in our model, including our approach to the calculation of the imaginary part of the QCD eikonal function which leads ultimately to a nonzero value for ρ. We give the results of our calculations for ρ, the slope parameter B, $\Delta\sigma$, and the pp and $\bar{p}p$ cross sections for $\sqrt{s}$ from 20 GeV to 10^5 GeV in Sec. III A; define the jet cross section $\sigma_{\rm jet}$, and present our results on $\sigma_{\rm jet}$, expected jet multiplicities, and fluctuations in Sec. III B; and conclude in Sec. III C with a brief discussion of uncertainties in the model.

II. THE MODEL

A. Theoretical background

We will work in the impact-parameter representation for the nucleon-nucleon scattering amplitude, neglecting spin. The pp and $\bar{p}p$ elastic-scattering amplitudes can then be represented as

$$f_{pp,\bar{p}p}(s,t)=i\int_0^\infty db\, b(1-e^{-\chi_{pp,\bar{p}p}(b,s)})J_0(b\sqrt{-t}) , \quad (1)$$

where s and t are the usual Mandelstam variables and J_0 is a Bessel function. The eikonal function $\chi(b,s)$ is complex:

$$\chi(b,s)=\chi^R(b,s)+i\chi^I(b,s) . \quad (2)$$

Our normalization is such that the elastic differential scattering cross section is given by

$$\frac{d\sigma}{dt}=\pi|f(s,t)|^2 . \quad (3)$$

With this normalization, the total, elastic, and inelastic scattering cross sections are

$$\sigma_{\rm total}(s)=4\pi\,\mathrm{Im}f(s,0)$$
$$=4\pi\int_0^\infty db\, b[1-\cos\chi^I(b,s)e^{-\chi^R(b,s)}] , \quad (4a)$$
$$\sigma_{\rm elastic}=2\pi\int_0^\infty db\, b|1-e^{-\chi(b,s)}|^2$$
$$=2\pi\int_0^\infty db\, b[1-2\cos\chi^I(b,s)e^{-\chi^R(b,s)}+e^{-2\chi^R(b,s)}] , \quad (4b)$$
$$\sigma_{\rm inelastic}=2\pi\int_0^\infty db\, b(1-e^{-2\chi^R(b,s)}) . \quad (4c)$$

As emphasized in our previous work,[6,7] the term $e^{-2\chi^R}$ in the expression for $\sigma_{\text{inelastic}}$ can be interpreted semiclassically as the probability that neither nucleon is broken up, and that there is no particle production, in a collision at impact parameter b. We have used this argument to determine the contribution of semihard parton-parton collisions to χ^R as summarized in Refs. 6 and 7 and in the following section. Our aim here is to use the known analyticity properties of the spin-averaged nucleon-nucleon scattering amplitude[13] to determine the QCD contribution to χ^I given χ^R_{QCD}.

The scattering amplitudes $f(s,t)$ defined in Eq. (1) can be expressed in terms of the usual Feynman amplitudes $F(s,t)$ by

$$F_{pp,\bar{p}p}(s,t)=8\pi i[s(s-4m^2)]^{1/2}[-if_{pp,\bar{p}p}(s,t)] . \quad (5)$$

The F's are analytic functions of s and t which are related by crossing symmetry and are simply different boundary values of a single analytic function $\mathcal{F}$. In particular, for $t=0$ (forward scattering),

$$F_{pp}(s,0)=\lim_{\epsilon\to 0}\mathcal{F}(E+i\epsilon,0) , \quad (6a)$$

$$F_{\bar{p}p}(s,0)=\lim_{\epsilon\to 0}\mathcal{F}(-E-i\epsilon,0) , \quad (6b)$$

where $E=(s-2m^2)/2m$. $\mathcal{F}(E,0)$ is a real-analytic function of E (Refs. 13 and 14). The factor $i[s(s-4m^2)]^{1/2}$ on the right-hand side of Eq. (5) is equal to $2m(m^2-E^2)^{1/2}$, and is an even, real-analytic function of E. Thus the functions $-if_{\pm}(s,0)$ defined by

$$-if_{\pm}(s,0)=\frac{-i}{2}[f_{\bar{p}p}(s,0)\pm f_{pp}(s,0)] \quad (7)$$

are even (odd) real-analytic functions and satisfy simple dispersion relations.[13]

If we work with the χ's instead of the f's and write

$$\chi_{\bar{p}p}=\chi_+ +\chi_- , \quad \chi_{pp}=\chi_+ -\chi_- , \quad (8)$$

we find that

$$-if_+(s,0)=\int_0^\infty db\, b(1-e^{-\chi_+}\cosh\chi_-) , \quad (9a)$$

$$-if_-(s,0)=\int_0^\infty db\, be^{-\chi_+}\sinh\chi_- . \quad (9b)$$

The required analytic properties of $f_{\pm}(s,0)$ are clearly satisfied if $\chi_+(s,b)$ and $\chi_-(s,b)$ are even (odd) real-analytic functions of E with the same cut structure as $f_{\pm}$, a result which is frequently used in parametrizations of the χ's in terms of powers of E or s, e.g., in Refs. 5 and 8–10. We will use a different approach in calculating χ_{QCD} since we found *ad hoc* parametrizations of this function to be unsatisfactory,[15] and will relate χ^I_{QCD} to χ^R_{QCD} using a dispersion relation.

To obtain a dispersion relation for $\text{Im}\chi_+(b,s)$ in terms of $\text{Re}\chi_+(b,s)$, we apply Cauchy's theorem to the even function

$$\phi(E)=\chi_+(b,E)/(m^2-E^2)^{1/2}, \quad s=2mE+2m^2 . \quad (10)$$

A standard construction[13,16,17] in which we ignore the singularities of χ_+ in the unphysical region $|E|<m$ (which are irrelevant at large values of s or E) gives the dispersion relation

$$\text{Im}\chi_+(b,E)=-\frac{2}{\pi}(E^2-m^2)^{1/2}\text{P}\int_m^\infty dE'\frac{E'}{(E'^2-m^2)^{1/2}}\times\frac{\text{Re}\chi_+(b,E'+i\epsilon)}{E'^2-E^2} . \quad (11)$$

We will be concerned only with high energies, and will be able to neglect m relative to E or E'. Taking this limit and changing variables from E to s, we obtain the dispersion relation we will use in the next section:

$$\chi^I_+(b,s)=-\frac{2s}{\pi}\text{P}\int_0^\infty ds'\frac{\chi^R_+(b,s')}{s'^2-s^2}, \quad s\gg m^2 . \quad (12)$$

The odd eikonal function satisfies a similar dispersion relation:

$$\chi^I_-(b,s)=-\frac{2s^2}{\pi}\text{P}\int_0^\infty ds'\frac{\chi^R_-(b,s')}{s'(s'^2-s^2)}, \quad s\gg m^2 . \quad (13)$$

It is useful to note here that these relations imply that a pure power-law term in χ at high energies can only be of the form $(se^{-i\pi/2})^\alpha$ in χ_+ or $i(se^{-i\pi/2})^\alpha$ in χ_-, that is, the phases are determined.

B. Model for the eikonal functions

We will write the eikonal functions $\chi_{pp,\bar{p}p}$ as sums of contributions from semihard QCD processes and soft interactions:

$$\chi(b,s)=\chi_{\text{soft}}(b,s)+\chi_{\text{QCD}}(b,s) . \quad (14)$$

In Refs. 6 and 7, we argued that $e^{-2\,\text{Re}\chi_{\text{QCD}}}$ is the probability that there are no semihard parton interactions in a nucleon-nucleon collision and showed from this assumption that $\text{Re}\chi_{\text{QCD}}$ is given in terms of the parton-parton scattering cross sections and the parton distributions in a nucleon by

$$\chi^R_{\text{QCD}}(b,s)=\text{Re}\chi_{\text{QCD}}(b,s)=\tfrac{1}{2}\sum_{ij}\frac{1}{1+\delta_{ij}}\int d^2b'\int dx_1\int dx_2\int_{Q^2_{\min}} d|\hat{t}|\frac{d\hat{\sigma}_{ij}}{d|\hat{t}|}f_i(x_1,|\hat{t}|,|\mathbf{b}-\mathbf{b}'|)f_j(x_2,|\hat{t}|,|\mathbf{b}'|) . \quad (15)$$

Here $\hat{s}$ and $\hat{t}$ are the Mandelstam variables for the parton-parton collision and $f_i(x,|\hat{t}|,b)dx\,d^2b$ is the number of partons of type i in the interval dx of the fractional longitudinal momentum x, and in the transverse area element d^2b a distance b from the initial line of flight of the proton.

We will assume that the f's factor

$$f_i(x,|\hat{t}|,b)\approx f_i(x,|\hat{t}|)\rho(b)\ , \tag{16}$$

where $f_i(x,|\hat{t}|)$, is the usual parton distribution in the proton and $\rho(b)$ is the probability density for finding the parton in the area d^2b at impact parameter b. This factorization is consistent with the usual parton picture and the QCD evolution of well-localization partons at small x. Then

$$\chi^R_{\rm QCD}(b,s)=\tfrac{1}{2}A(b)\sigma^R_{\rm QCD}(s)\ , \tag{17}$$

where $\sigma^R_{\rm QCD}$ is the usual (real) parton-level cross section

$$\sigma^R_{\rm QCD}(s)=\sum_{i,j}\frac{1}{1+\delta_{ij}}\int_0^1 dx_1\int_0^1 dx_2\int_{Q^2_{\rm min}} d|\hat{t}|\frac{d\hat{\sigma}_{ij}}{d|\hat{t}|}f_i(x_1,|\hat{t}|)f_j(x_2,|\hat{t}|)\theta\left[\frac{\hat{s}}{2}-|\hat{t}|\right]\ , \tag{18}$$

and $A(b)$ is the overlap density for the protons at impact parameter b:

$$A(b)=\int d^2b'\rho(|\mathbf{b}-\mathbf{b}'|)\rho(b')\ , \tag{19a}$$

$$2\pi\int_0^\infty db\ bA(b)=1\ . \tag{19b}$$

The even and odd parts of $\chi^R_{\rm QCD}$ are equal to one-half of the sum and the difference of the QCD cross sections in Eq. (18) for $\bar{p}p$ and pp scattering. These cross sections differ only because of the different weighting of the quark-antiquark annihilation cross section in the two cases. However, the annihilation cross section is quite small, decreases rapidly with increasing s, and can be neglected at CERN ISR energies and above. We will therefore simply identify the QCD contribution to χ^R_+ with $\chi^R_{\rm QCD}$ calculated for pp scattering, and neglect the very small QCD contribution to χ^R_-. Then, applying the dispersion relation in Eq. (12) and evaluating the dispersion integral explicitly, we obtain the imaginary part of $\chi_{\rm QCD}$:

$$\chi^I_{\rm QCD}={\rm Im}\chi_{\rm QCD}(b,s)=\tfrac{1}{2}A(b)\sigma^I_{\rm QCD}(s)\ , \tag{20}$$

where

$$\sigma^I_{\rm QCD}(s)=-\frac{1}{\pi}\sum_{ij}\frac{1}{1+\delta_{ij}}\int_0^1 dx_1\int_0^1 dx_2\int_{Q^2_{\rm min}}^\infty d|\hat{t}|\frac{d\hat{\sigma}_{ij}}{d|\hat{t}|}f_i(x_1,|\hat{t}|)f_j(x_2,|\hat{t}|)\ln\frac{||\hat{t}|+\hat{s}/2}{|\hat{t}|-\hat{s}/2|},\quad \hat{s}=x_1x_2s\ . \tag{21}$$

While $\chi_{\rm QCD}$ gives the dominant contribution to the even eikonal function at very high energies, we still need a large "soft" contribution to describe pp and $\bar{p}p$ scattering at ISR energies. We will parametrize the even contribution as

$$\chi_{+,\rm soft}(b,s)=\tfrac{1}{2}A_+(b)\sigma_{\rm soft}\ , \tag{22}$$

with

$$\sigma_{\rm soft}=\sigma_0+\frac{a}{s^\alpha}e^{i\alpha\pi/2}\ . \tag{23}$$

The second term can be interpreted as a Regge-exchange term (f exchange). We will treat the constants $\sigma_0=\sigma_0^R+i\sigma_0^I$, a, and α as adjustable parameters.

We expect the geometric factor $A_+(b)$ in Eq. (22) to be different from the factor $A(b)$ in $\chi_{\rm QCD}$. The soft interactions mainly involve interactions of valence quarks, while the QCD term is dominated by gluons. The gluons are presumably distributed around the quarks, and thus should exhibit a somewhat different spatial distribution. We will assume that the distribution of valence quarks is similar to the proton's charge distribution as in the Durand-Lipes-Chou-Yang model:[18,19]

$$\rho_+(b)\approx\frac{1}{(2\pi)^2}\int d^2k_\perp G_E(k_\perp^2)e^{i\mathbf{k}_\perp\cdot\mathbf{b}}\ , \tag{24a}$$

$$G_E(k_\perp^2)=(1+k_\perp^2/\nu^2)^{-2}\ , \tag{24b}$$

where G_E is the proton form factor, but will take the parameter ν as adjustable. With this assumption,

$$A_+(b)=\frac{\nu_+^2}{12\pi}\frac{1}{8}(\nu_+b)^3K_3(\nu_+b)\ . \tag{25}$$

We will further assume the gluons are distributed around the valence quarks in a Yukawa distribution with Fourier transform

$$(1+k_\perp^2/\mu^2)^{-1}\ . \tag{26}$$

The gluon distribution in a proton is the convolution of the distribution around quarks with the quark distribution and is given in momentum space by

$$G(k_\perp^2)=(1+k_\perp^2/\nu_+^2)^{-2}(1+k_\perp^2/\mu^2)^{-1}\ . \tag{27}$$

A straightforward calculation then gives

$$A(b)=\frac{\nu_+^2}{12\pi}\frac{1}{(1-\eta)^2}\left[\frac{1}{8}(\nu_+b)^3K_3(\nu_+b)-\frac{3}{2}\frac{\eta}{1-\eta}(\nu_+b)^2K_2(\nu_+b)\right.$$
$$\left.+\frac{9\eta^2}{(1-\eta)^2}(\nu_+b)K_1(\nu_+b)-\frac{24\eta^3}{(1-\eta)^3}[K_0(\nu_+b)-K_0(\mu b)]+\frac{3\eta^3}{(1-\eta)^2}(\mu b)K_1(\mu b)\right]\ , \tag{28}$$

where $\eta=\nu_+^2/\mu^2$. We will use this distribution for all partons in calculating $\chi_{\rm QCD}$ since sea quarks originate with gluons, and dominate the quark distributions at small x.

The odd eikonal $\chi_-(b,s)$ is determined by the long-range Regge exchanges, specifically the exchanges of ρ and ω trajectories, and should vary roughly as $s^{-1/2}$. We will parametrize it as

$$\chi_-(b,s)=\tfrac{1}{2}A_-(b)\frac{R}{\sqrt{s}}e^{-i\pi/4}\ , \tag{29}$$

where the phase is again determined by analyticity, and

$$A_-(b)=\frac{\nu_-^2}{12\pi}\frac{1}{8}(\nu_- b)^3K_3(\nu_- b)\ . \tag{30}$$

Because of the long range of the Regge exchanges, we expect the characteristic radius ν_-^{-1} of the odd exchanges to be larger than the parameter ν_+^{-1} in Eq. (25).

III. RESULTS

A. Cross sections, ρ, and B

We have completely specified the eikonal functions above. The general expressions in Eqs. (1)–(4) now allow us to calculate the elastic differential cross section, the total, elastic, and inelastic cross sections, the ratio ρ of the real to the imaginary parts of the forward-scattering amplitude,

$$\rho=\mathrm{Re}f(s,0)/\mathrm{Im}f(s,0)\ , \tag{31}$$

and the forward slope parameter B given by

$$B=\frac{d}{dt}\left[\ln\frac{d\sigma}{dt}\right]\Bigg|_{t=0}\ . \tag{32}$$

In evaluating $\chi_{\rm QCD}$, we have used the QCD-evolved quark and gluon distribution functions of Eichten, Hinchliffe, Lane, and Quigg[20] (set 1 with $\Lambda_{\overline{\rm MS}}=200$ MeV, where MS denotes the modified minimal-subtraction scheme). We obtain a reasonable fit to the measured values[21–26] of the quantities above using the parameters

$$\sigma_0^R=130\ \mathrm{GeV}^{-2},\quad \nu_+^2=0.77\ \mathrm{GeV}^{-2},\quad a=440\ \mathrm{GeV}^{-2}\ ,$$
$$\sigma_0^I=-3\ \mathrm{GeV}^{-2},\quad \nu_-^2=0.35\ \mathrm{GeV}^{-2},\quad R=140\ \mathrm{GeV}^{-2}\ , \tag{33}$$
$$a=0.7,\quad \mu^2=0.88\ \mathrm{GeV}^{-2},\quad Q_{\rm min}^2=3.2\ \mathrm{GeV}^2\ ,$$

but have not attempted to obtain a "best" fit. Our results are shown in Figs. 1–5 below.

The calculated cross sections $\sigma_{\rm total}$ and $\sigma_{\rm elastic}$ are shown in Fig. 1 along with the measured cross-section data[21] for $\sqrt{s}$ up to 10^5 GeV. The cosmic-ray cross-section data[22] shown in Fig. 1 are probably to be regarded as giving lower limits on the actual high-energy NN cross section,[27] and are somewhat dependent on the model used to convert from p-air to pp cross sections.[28,29] The calculated cross sections shown in Fig. 1 are significantly higher at cosmic-ray energies than those published earlier.[6,7] The difference results primarily from our attempt here to fit the large value of ρ at 546 GeV reported by the UA4 group.[26] This requires a more rapid increase in $\sigma_{\rm QCD}$ than is favored by the cross-section data alone over the ISR–CERN-collider region, and necessitated a somewhat different treatment of the kinematic cutoffs than was used in Ref. 7. However, the experimental situation is not completely clear. A preliminary measurement of $\sigma_{\rm tot}$ reported since our fit was done gives the value[30] $\sigma_{\rm total}=75.5\pm5.7$ mb at $\sqrt{s}=1.8$ TeV compared to the calculated value of 82 mb in Fig. 1. This lower cross section agrees well with our earlier calculations, but would probably be inconsistent with the UA4 value for ρ at 546 GeV.

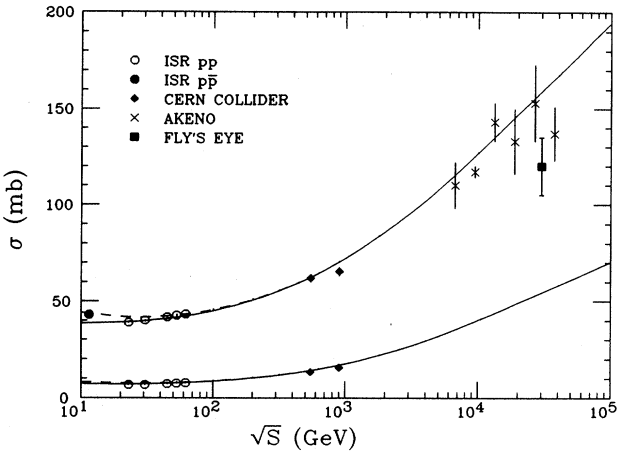

FIG. 1. The calculated pp and $\bar{p}p$ cross sections given by the QCD-driven diffraction scattering model, as functions of the total center-of-mass energy $\sqrt{s}$. Top curves: $\sigma_{\rm total}$. Bottom curves: $\sigma_{\rm elastic}$. The $\bar{p}p$ and pp cross sections are shown by dashed and solid curves, respectively. The data are from Refs. 21 and 22. Only representative points are shown at the lower energies.

The difference of the total cross sections[23] $\Delta\sigma=\sigma_{\bar{p}p}-\sigma_{pp}$ is shown in Fig. 2. This difference disappears very rapidly as expected, and is negligible above the ISR energy range.

In Fig. 3 we compare the differential $\bar{p}p$ scattering cross section calculated at 546 GeV with the UA4 data[24] at that energy. The general agreement of the model with the data is a test of the geometrical aspects of the model. We note in this connection that the smearing out of the gluon (or parton) distribution relative to the soft-valence-quark distribution which is represented by the extra factor in Eq. (27) is quite important in getting a good fit to $d\sigma/dt$ over 4 orders of magnitude in this quantity. The discrepancies between the calculated and measured values of $d\sigma/dt$ at large values of $|t|$ are a common problem in simple models of this type, and can be removed by small changes in the eikonal function (see, e.g., Ref. 9 or Glauber and Velasco[31]). Figure 3 also shows the prediction of the present model for $d\sigma/dt$ at the energy of the proposed Superconducting Super Collider: 40 TeV.

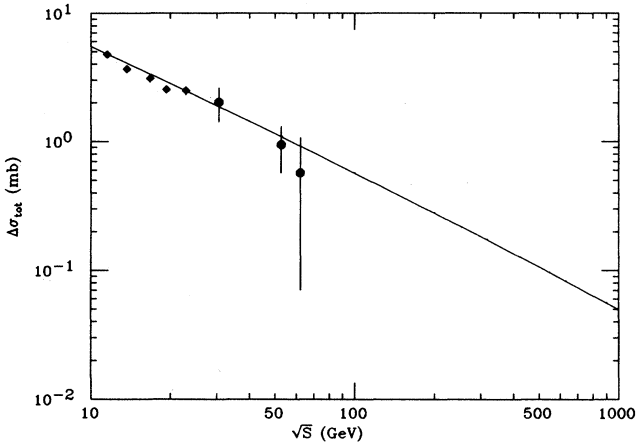

FIG. 2. The total-cross-section difference $\Delta\sigma=\sigma_{\bar{p}p}-\sigma_{pp}$ calculated with the parameters in Eq. (33). Only the lowest-energy point was fitted. The data are representative points from Ref. 23.

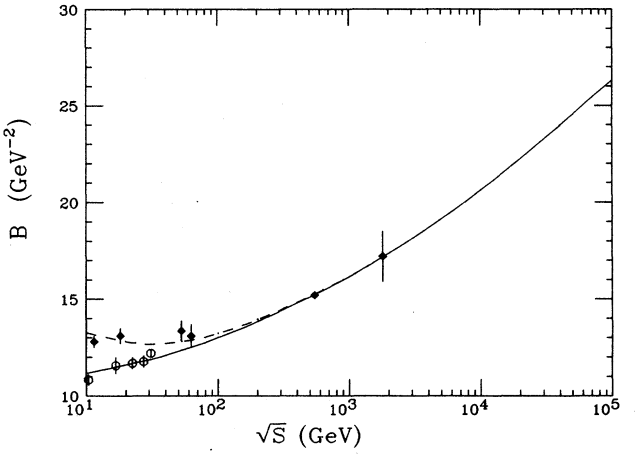

FIG. 4. The pp and $\bar{p}p$ forward slope parameters $d/dt(\ln d\sigma/dt)_{t=0}$ calculated with the QCD-driven model. $\bar{p}p$: solid diamonds and dashed curve. pp: open circles and solid curve. The data are from Ref. 25. Only representative points are shown at the lower energies.

In Fig. 4 we show the forward slope parameter for pp and $\bar{p}p$ scattering.[25] We predict a continuing increase in B, that is, a steepening of the forward diffraction peak in $d\sigma/dt$. This steepening is clearly evident in Fig. 3 in the comparison of the differential cross sections calculated for $\sqrt{s}$ equal to 546 GeV and 40 TeV, and pushes the predicted first diffraction minimum to smaller $|t|$ at the higher energy.

One of the most interesting results is one which appears in Fig. 5, where we show the ratio ρ of the real to the imaginary part of the forward-scattering amplitude, a quantity which can be measured through the interference of the strong-interaction part of the scattering with the Coulomb scattering at very small angles.[17,26] The recent UA4 measurement of ρ at $\sqrt{s}=546$ GeV gave an unexpectedly large value for this quantity, but one which we are able to fit reasonably well.

The rapid increase in ρ in our calculations is associated with the rapid increase in the QCD contribution $\chi^I_{\rm QCD}$ to the imaginary part of the even eikonal function, as is clearly evident from Fig. 6. The sign, magnitude, and energy dependence of $\chi^I_{\rm QCD}$ are all determined by the relations in Eqs. (20) and (21) once the QCD parameters and $A(b)$ are specified. We calculated $\sigma^I_{\rm QCD}$ directly from Eq. (21) using the standard parton distribution functions

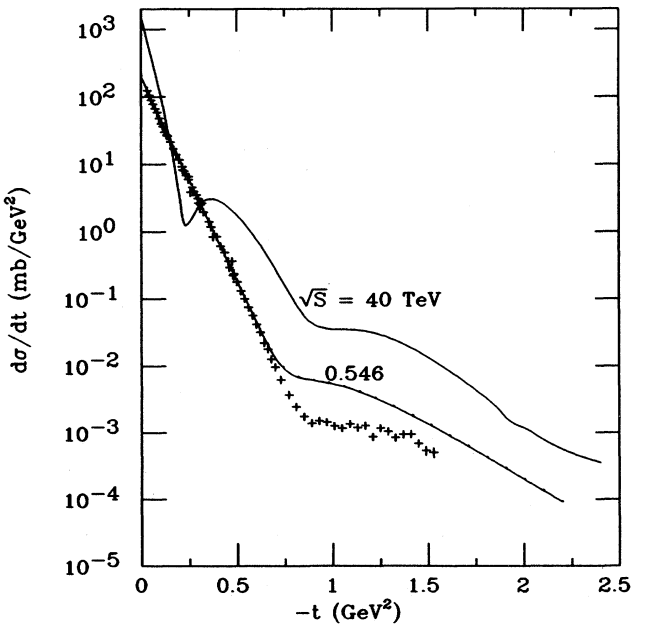

FIG. 3. The differential $\bar{p}p$ scattering cross sections $d\sigma/dt$ calculated at $\sqrt{s}=546$ GeV and 40 TeV. The data at 546 GeV are from Ref. 24.

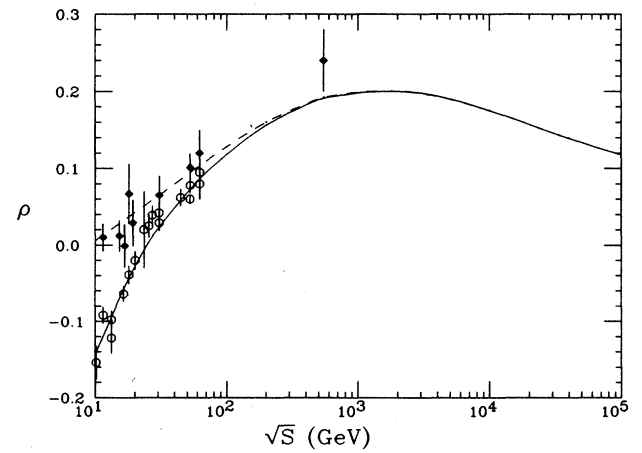

FIG. 5. The ratios $\rho=\mathrm{Re}f(0)/\mathrm{Im}f(0)$ for pp and $\bar{p}p$ scattering calculated with the QCD-driven model. $\bar{p}p$: solid diamonds and dashed curve. pp: open circles and solid curve. The data are from Ref. 26. Only representative pp data are shown.

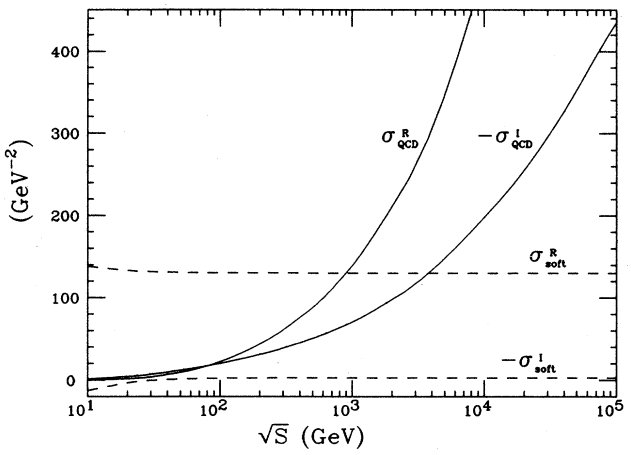

FIG. 6. The elementary parameters which enter the even eikonal function $\chi_+(b,s)=\frac{1}{2}[\sigma^R_{soft}A_+(b)+\sigma^R_{QCD}A(b)]+(i/2)[\sigma^I_{soft}A_+(b)+\sigma^I_{QCD}A(b)]$. The cross sections σ^R_{QCD} and σ^I_{QCD} were calculated using Eqs. (18) and (21), respectively, with $Q_{min}=3.2$ (GeV/c)^2. σ_{soft} is defined in Eq. (23).

of Eichten, Hinchliffe, Lane, and Quigg, set 1 (Ref. 20). The only free parameter in this calculation is Q^2_{min}, which is adjusted within the model to fit $\sigma_{total}(\bar{p}p)$ at 546 GeV.

The connection of the increase in ρ to the increase in the QCD contribution to the eikonal function was apparently first noted by Dias de Deus and Kwieciński,[9] who parametrized the energy dependence of the QCD term in their eikonal function as a power $(s-s_0)^\alpha$, and then made the replacement $(s-s_0)\to e^{-i\pi/2}(s-s_0)$ required by analyticity. Their QCD contribution to χ_+ was unfortunately too small, and their prediction for ρ was consequently too small, also. One of us[15] subsequently used a similar parametrization for the χ_{QCD} used in our previous work,[6,7] and obtained results for ρ at 546 GeV as good as, or better than, that shown in Fig. 5. However, the results were fairly sensitive to the details of the parametrization used. We subsequently adopted the present, unambiguous approach based on dispersion relations for χ. The parametrization problem was handled in a different way by Margolis *et al.*[10] in their recent paper on QCD effects on forward scattering amplitudes by using analytic parametrizations of the parton distribution functions, and making the replacement $s\to se^{-i\pi/2}$ in the final result for σ^R_{QCD}. Our results agree quite well with theirs. We would emphasize, however, that the calculation of σ^I_{QCD} is no more complicated in our approach than the calculation of σ^R_{QCD} and allows us to use properly evolved parton distribution functions in both calculations.

It is also clear from Fig. 6 that parton-parton scattering drives the increase in σ_{total}, $\sigma_{elastic}$, $\sigma_{inelastic}$, and B through the increase in χ^R_{QCD} or σ^R_{QCD}, with the parton processes giving the dominant contribution to the eikonal function above about 900 GeV. At sufficiently high energies, σ_{total} and $\sigma_{elastic}$ would nominally approach "black-disk" cross sections with $\sigma_{total}\propto\ln^2 s$, but the increasing density of partons in the proton at smaller x will eventually lead to nonlinear effects[32] which may slow the approach to an asymptotic unit.

B. Jet cross sections and fluctuations

We define the inclusive jet cross section $\sigma_{jet}(Q^2)$ as the part of the pp cross section which corresponds to events with at least one semihard parton-parton scattering with a minimum momentum transfer $|\hat{t}|_{min}=Q^2$, irrespective of any soft processes which may occur. Recall that the semiclassical probability that there is *no* parton-parton scattering in a pp collision at impact parameter b is $e^{-2\chi^R_{QCD}}$, where χ^R is the real part of the eikonal function. Using this observation, we may write the inelastic cross section as

$$\begin{aligned}\sigma_{inelastic}&=2\pi\int_0^\infty db\, b(1-e^{-2\chi^R_{soft}-2\chi^R_{QCD}})\\&=2\pi\int_0^\infty db\, b(1-e^{-2\chi^R_{QCD}(Q^2)})\\&\quad+2\pi\int_0^\infty db\, b(1-e^{-2\chi^R_{soft'}})e^{-2\chi^R_{QCD}(Q^2)}\\&=\sigma_{jet}+\sigma_{soft}\,,\end{aligned}\tag{34}$$

where[7]

$$\sigma_{jet}(s,Q^2)=2\pi\int_0^\infty db\, b(1-e^{-2\chi^R_{QCD}(Q^2)})\,.\tag{35}$$

Here $\chi^R_{QCD}(Q^2)$ is defined by Eqs. (17) and (18) with a cutoff Q^2 replacing Q^2_{min}, and $\chi^R_{soft'}$ includes the QCD contributions with $Q^2_{min}\le|\hat{t}|\le Q^2$. The cross section σ_{soft} corresponds to processes with *no* QCD jets with $|\hat{t}|>Q^2$; σ_{jet} contains all other types of events, all of which (by construction) contain jets.[33]

We emphasize that the definition of σ_{jet} in Eq. (35) differs from the (incorrect) definition $\sigma_{jet}=\sigma^R_{QCD}$ used by some authors. The two definitions are equivalent only if χ^R_{QCD} is sufficiently small. The definition above takes proper account of the fact that there may be multiple semihard parton-parton interactions in a single pp collision.[34] Note that σ_{jet} is independent of $\chi^R_{soft'}$ but that the soft or jet-free cross section is strongly suppressed for χ^R_{QCD} large. (Capella, Tran Thanh Van, and Kwieciński[8] use an equivalent definition of σ_{jet}, but use a different (inclusive) definition of the soft cross section. Their parametrizations of χ_{soft} and χ_{QCD} also have quite different energy dependences from ours.)

The jet cross section is shown in Fig. 7 for several choices of the minimum momentum transfer Q allowed in the calculation of σ^R_{QCD}, Eq. (18). We also show the inclusive jet cross section σ^R_{QCD} for comparison. In Fig. 8 we compare the jet cross section for $Q=3$ GeV/c with the full inelastic cross section. It is evident that σ_{jet} constitutes most of the $\sigma_{inelastic}$ at high energies.

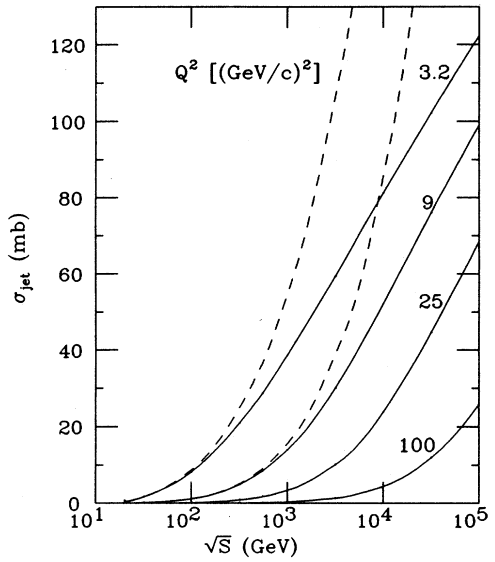

FIG. 7. Predictions for the inclusive pp or $\bar{p}p$ jet cross section σ_{jet} as a function of the total center-of-mass energy $\sqrt{s}$, for several values of the cutoff Q^2 in Eq. (18). Solid curves: σ_{jet} from Eq. (35). Dashed curves: the inclusive parton-level cross section σ_{QCD} from Eq. (18).

We emphasize that the jets considered here are not extremely hard. The softer jets, for example, those which fill in between the upper curves in Fig. 7, are clearly not distinguishable as UA1-type minijets[3,4] using standard jet algorithms, but still represent the production of hadrons at traverse momenta which are quite large by normal hadronic standards. The UA1 minijet analysis picks up multiparticle jets with total transverse energies in the jet cone down to 5 GeV. As pointed out by Pancheri and Srivastava,[4] this corresponds to a minimum transverse energy of ~ 3 GeV for distinguishable jets when account is taken of the transverse energy in the underlying event. We compare the UA1 data with the jet cross section calculated for $Q=3$ GeV/c in Fig. 8. The calculated cross section is somewhat low, but clearly has the correct energy dependence. A change in Q^2 to 7 (GeV/c)^2 gives excellent agreement with the data. However, we have not attempted a real fit including the effects of jet fragmentation and the underlying event.

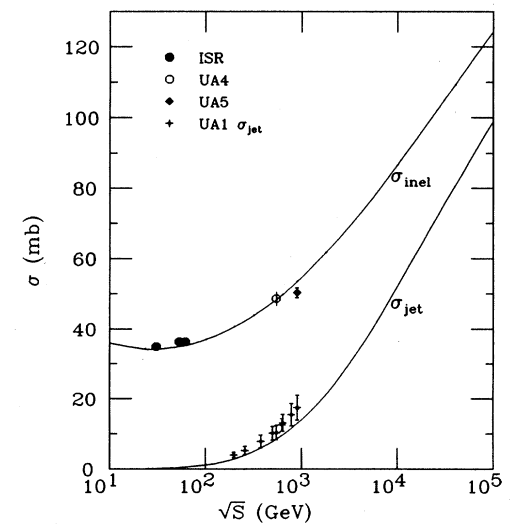

FIG. 8. Comparison of the jet cross section σ_{jet} for $Q=3$ GeV/c with the full inelastic pp scattering cross section $\sigma_{\text{inelastic}}$. The UA1 minijet data from Ref. 3 are shown for comparison with σ_{jet}. The data on $\sigma_{\text{inelastic}}$ are from Ref. 21.

The average number of parton-parton scatterings with $|\hat{t}|>Q^2$ in a pp collision at impact parameter b is[6,7]

$$n(b,s,Q^2)=\sigma^R_{\text{QCD}}(s,Q^2)A(b) =2\chi^R_{\text{QCD}}(b,s,Q^2)\ , \tag{36}$$

where σ^R_{QCD} is the parton-level cross section in Eq. (18) evaluated with a cutoff Q^2 rather than Q^2_{min}. Since the parton scatterings in our model are independent, the relative probability of having n scatterings in a collision at impact parameter b is given by a Poisson distribution with an average number of scatterings equal to $n(b,s,Q^2)$:

$$P_n(b,s,Q^2)=\frac{1}{n!}[n(b,s,Q^2)]^n e^{-n(b,s,Q^2)}\ . \tag{37}$$

The average probability distribution for n parton scatterings averaged over *all* inelastic events is then

$$P_n(s,Q^2)=\frac{2\pi}{\sigma_{\text{inelastic}}}\frac{1}{n!}\int_0^\infty db\ b[n(b,s,Q^2)]^n e^{-n(b,s,Q^2)}\ , \quad n\geq 1\ , \tag{38a}$$

$$P_0(s,Q^2)=\frac{2\pi}{\sigma_{\text{inelastic}}}\int_0^\infty db\ b(1-e^{-2\chi^R_{\text{soft}'}})e^{-n(b,s,Q^2)} =\frac{\sigma_{\text{soft}}}{\sigma_{\text{inelastic}}}\ , \tag{38b}$$

$$\sum_{n=1}^\infty P_n(s,Q^2)=\frac{\sigma_{\text{jet}}}{\sigma_{\text{inelastic}}}=1-\frac{\sigma_{\text{soft}}}{\sigma_{\text{inelastic}}}\ . \tag{38c}$$

The factors $e^{-n(b,s,Q^2)}$ and $(1-e^{-2\chi^R_{\text{soft}'}})$ in expression for P_0 are, respectively, the Poisson probability that there are no hard collisions, and the probability that there *is* a soft collision at impact parameter b.

The average jet multiplicity is given, using Eqs. (19a) and (38a), by

$$\bar{n}_{\text{jets}}(s,Q^2)=\sum_{n=1}^\infty 2nP_n(s,Q^2) =2\sigma^R_{\text{QCD}}(s,Q^2)/\sigma_{\text{inelastic}}\ . \tag{39}$$

That is, $\bar{n}_{\text{jets}}$ is just the ratio of the inclusive jet cross sec-

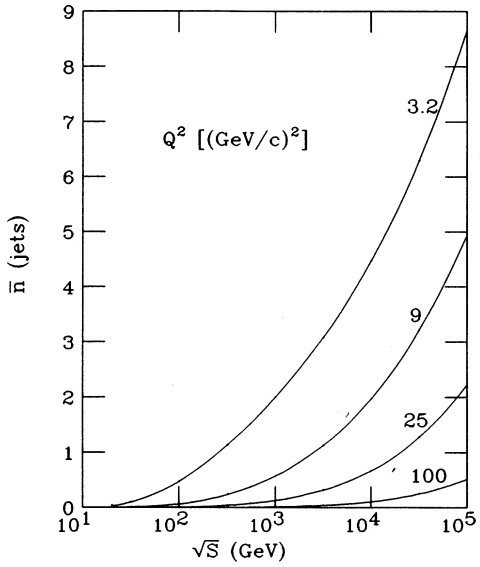

FIG. 9. Predictions for the average number of jets produced in a pp or $\bar{p}p$ collision as a function of $\sqrt{s}$, shown for several values of the minimum invariant momentum transfer $|\hat{t}|=Q^2$ in the parton-parton scattering.

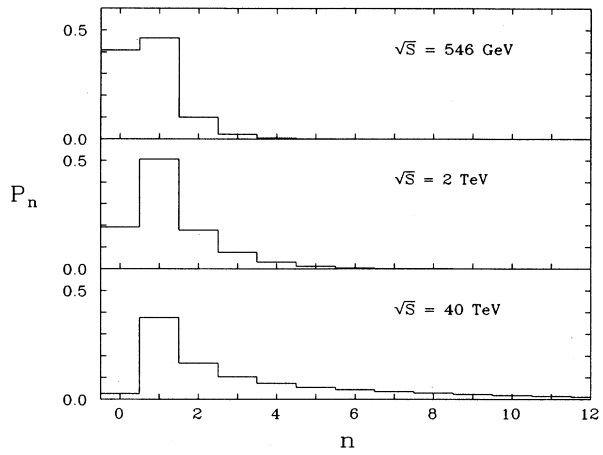

FIG. 10. The probability distribution P_n for having n semihard parton-parton collisions or $2n$ jets in a pp or $\bar{p}p$ collision, for various values of $\sqrt{s}$ and the momentum-transfer cutoff $Q^2=3.2$ (GeV/c)^2 used in the calculations in Figs. 1–6.

tion to the total inelastic cross section, with an extra factor of 2 because each semihard or hard parton scattering produces two jets. The average jet multiplicity $\bar{n}_{\text{jets}}(s,Q^2)$ is shown in Fig. 9 for several choices of Q^2. The prediction of the model for the energy of the proposed superconducting supercollider, 40 TeV, is that an "average" event will contain about four jets at least as hard as the UA1 minijets, and that a large fraction of events will contain much harder jets. Thus typical events will involve transverse momenta much larger than the typical scale of $\sim$400 MeV/c characteristic inelastic interactions at low energies, and we may expect the events to be rather "noisy," that is, to contain large fluctuations in transverse momenta and particle multiplicities. However, as noted above, most of the semihard jets will not be observable as well-defined jets using standard jet-finding algorithms.[4]

The fact that the fluctuations in the jet multiplicities are very large may be seen qualitatively from Fig. 10, where we plot $P_n(s,Q^2_{\text{min}})$ as a function of n, the number of parton collisions or one-half the number of jets. The probability of having no jets in an event decreases rapidly with increasing energy as expected from Eq. (38b) and Fig. 8. Because of the impact-parameter averaging in Eq. (38a), the distribution P_n for $n \geq 1$ is very non-Poissonian, with a rather slowly falling large-n tail at high energies, and no peak at the average number of collisions, $\bar{n} \approx 3$ for $\sqrt{s}=40$ TeV. The size of the fluctuations is likely to be significant for hadronic multiplicity distributions. Preliminary calculations of multiplicity distributions which include fragmentation of the QCD jets considered above, as well as soft production of hadrons in the remaining "beam jets" through string fragmentation, appear to give a satisfactory description of the existing data including the energy dependence and the broadening of the Koba-Nielsen-Olesen scaling distribution, that is, the increase in multiplicity fluctuations with energy.

C. Conclusions and remarks

Overall, we find the agreement of our simple model with the extant data on pp and $\bar{p}p$ scattering as shown in Figs. 1–5 to be quite striking. The semihard parton scattering processes appear to account in a reasonable way for the observed energy dependence in the cross sections and the ρ and B parameters, and the fit to the differential pp scattering cross section is quite good over 4 orders of magnitude in this quantity. The calculated jet cross sections behave as expected from the UA1 minijet data,[3] and are in essential agreement with the results of Pancheri and Srivastava[4] who fit the UA1 data including the effects of the underlying soft processes in their analysis.

The model has two main areas of uncertainty. The first is in the treatment of the soft part of the eikonal function, and the merging of the soft and hard contributions. The second is concerned with the semihard interactions, particularly in the choice of the transverse-momentum cutoff Q_{min}, the neglect of higher-order QCD effects, and the choice of parton distribution functions. The main geometrical aspects of the model seem to be well established, though the factorization assumption for χ will presumably fail in the circumstance that a few partons carry all the momentum of the proton. The diffraction structure in $d\sigma/dt$ seen in Fig. 3, and seen also in the pp polarizations at lower energies, was *predicted* 20 years ago[18,19] using the same model for the b dependence of χ_{soft}, and is described essentially correctly for $\sqrt{s}$ from 8 to 630 GeV, the highest energy at which $d\sigma/dt$ has been measured.

The use of a *sharp* cutoff Q^2_{min} in the $\hat{t}$ integration in Eqs. (18) and (21) is largely irrelevant. It is introduced

partly to set the scale of semihard interactions, and partly to avoid the singularity in the forward parton-parton scattering cross sections. Except for the slow variation of α_s and the parton distribution functions with $|\hat{t}|$, we would obtain the same result for the $\hat{t}$ integration if we smoothed out the parton-parton scattering cross sections for $\hat{t}\to 0$ by replacing the singular, small-$\hat{t}$ terms $1/\hat{t}^2$ which appear there by $1/(Q^2_{\min}-\hat{t})^2$, with the same $Q_{\min}$. The choice of $Q_{\min}$ is restricted by the condition $Q_{\min} > \nu_+$ necessary for a parton to be confined laterally in the parent proton, and by the requirement that it be large enough in magnitude that perturbation theory can be expected to hold approximately. Both conditions are satisfied by our parameters. However, the effect of higher-order QCD contributions has not been explored.

The problem of merging the soft and hard contributions is more difficult. Some trade-off is clearly possible in the division of the energy dependence of χ between the soft and hard contributions. The leading contributions to both involve different limits of the same class of Feynman graphs in perturbative QCD, and should join smoothly. We have chosen to use a simple Regge description for χ_{soft} which *decreases* to a constant value with increasing $\sqrt{s}$, and then adjust $Q_{\min}$ to fit the rise in σ_{total} from ISR to the CERN-collider energies, i.e., $\sqrt{s}$ from 30–60 GeV to 900 GeV. We could shift some of the *increasing* energy dependence of χ to our parametrization of χ_{soft} as is done, for example, by Capella *et al.*,[8,12] and compensate by increasing the value of $Q_{\min}$. However, the rapid increase in ρ from its values at the ISR to the large value obtained in the UA4 measurement at $\sqrt{s}=546$ GeV, favors the rapid increase in χ characteristic of our model relative the much slower increase given, e.g., by the dual parton model (compare our Fig. 5 with Fig. 2 of Dias de Deus and Kwieciński, Ref. 9).

The energy dependence of χ_{QCD} results from the accessibility of smaller values of x, the fraction of the proton or antiproton momentum carried by a parton, at larger values of $\sqrt{s}$, coupled with the rapid growth of the parton distributions at small x. For example, the gluon distribution function increases more rapidly than x^{-1} for $x\to 0$ (Ref. 20), and small-x, semihard gluon-gluon interactions give the dominant contributions to χ_{QCD} at high energies. Unfortunately for our purposes, the gluon distribution function is not well known, and is not measured at all at the very small x's most relevant at high energies. We used the distribution functions of Eichten, Hinchliffe, Lane, and Quigg[20] in our calculations. Other choices for the distribution functions can give results for χ_{QCD} which differ substantially at large $\sqrt{s}$ from the χ_{QCD} obtained here. Although the differences are reduced in the cross sections, the actual behavior of the gluon distributions at small x remain a major uncertainty in the model, and one that will not be settled without better measurements.

ACKNOWLEDGMENTS

This work was supported in part by the U.S. Department of Energy under Contract No. DE-AC02-76ER00881. One of the authors (L.D.) would like to thank the Aspen Center for Physics for its hospitality while parts of this work were done.

[1]D. Cline, F. Halzen, and J. Luthe, Phys. Rev. Lett. **31**, 491 (1973); S. D. Ellis and M. B. Kislinger, Phys. Rev. D **9**, 2027 (1974); F. Halzen, Nucl. Phys. **B92**, 404 (1975); N. G. Antoniou, C. Chiou-Lahanas, S. D. P. Vlassopulos, and E. Zevgalatakos, Phys. Lett. **93B**, 472 (1980); F. Halzen and F. Herzog, Phys. Rev. D **30**, 2326 (1984).

[2]T. K. Gaisser and F. Halzen, Phys. Rev. Lett. **54**, 1754 (1985); G. Pancheri and Y. N. Srivastava, in *Physics Simulations at High Energy,* edited by V. Barger, T. Gottschalk, and F. Halzen (World Scientific, Singapore, 1987), pp. 56–76.

[3]F. Ceradini, in *Proceedings of the International Europhysics Conference on High Energy Physics,* Bari, Italy, 1985, edited by L. Nitti and G. Preparata (Laterza, Bari, Italy, 1985); C. E. Wultz, in *Hadrons, Quarks, and Gluons,* proceedings of the XXII Rencontre de Moriond, Les Arcs, France, 1987, edited by J. Tran Thanh Van (Editions Frontières, Gif-sûr-Yvette, France, 1987), pp. 235–241; C. Albajar, in *Physics Simulations at High Energy* (Ref. 2), pp. 39–55; A. Norton, in *Multiparticle Production,* edited by R. C. Hwa and Q.-B. Xie (World Scientific, Singapore, 1988), pp. 87–113; C. Albajar *et al.*, Nucl. Phys. **B309**, 405 (1988).

[4]G. Pancheri and Y. N. Srivastava, Phys. Lett. B **182**, 199 (1986); in *Multiparticle Production* (Ref. 3), pp. 364–378.

[5]P. l'Heureux, B. Margolis, and P. Valin, Phys. Rev. D **32**, 1681 (1985); B. Margolis and P. Valin, in *Physics Simulations at High Energy* (Ref. 3), pp. 178–185.

[6]L. Durand and H. Pi, in *Physics Simulations at High Energy* (Ref. 3), pp. 166–177; L. Durand and H. Pi, Phys. Rev. Lett. **58**, 303 (1987). Equation (12) of this paper contains an extra factor $A(b)$, and is missing an overall factor 2.

[7]L. Durand and H. Pi, in *Multiparticle Production* (Ref. 3) pp. 298–319; L. Durand, in *Hadrons, Quarks, and Gluons* (Ref. 3), pp. 253–259.

[8]A. Capella, J. Tran Thanh Van, and J. Kwieciński, Phys. Rev. Lett. **58**, 2015 (1987); J. Kwieciński, in *Hadrons, Quarks, and Gluons* (Ref. 3), pp. 243–252.

[9]J. Dias de Deus and J. Kwieciński, Phys. Lett. B **196**, 537 (1987).

[10]B. Margolis, P. Valin, M. M. Block, F. Halzen, and R. S. Fletcher, Phys. Lett. B **213**, 221 (1988).

[11]L. Durand, in *Proceedings of the Summer Study on the Deisgn and Utilization of the Superconducting Super Collider,* Snowmass, Colorado, 1984, edited by R. Donaldson and J. Morfin (Division of Particles and Fields of the APS, New York, 1985), p. 258. The simple additive model for total cross sections used in Refs. 1, $\sigma_{\text{total}}\approx\sigma_0+\sigma_{\text{QCD}}$ with σ_0 constant and σ_{QCD} the parton-level cross section, violates partial-wave unitarity badly at high energies.

[12]A different point of view on the energy dependence of the cross sections appears in Refs. 8 and 9. Those authors ascribe much of the energy dependence to soft processes. These are calculated in the dual parton model with a leading Regge intercept for the Pomeron $\alpha_P(0)>1$. The QCD processes are relatively less important.

[13]R. J. Eden, P. V. Landshoff, D. I. Olive, and J. C. Polkinghorne, *The Analytic S Matrix* (Cambridge University

Press, Cambridge, England, 1966); R. J. Eden, *High Energy Collisions of Elementary Particles* (Cambridge University Press, Cambridge, England, 1967).

[14]A real-analytic function $f(z)$ is analytic in a region R which contains a segment of the real axis, and is real on that segment. This implies that $f^*(z)=f(z^*)$ for z in R. $\mathcal{F}(E,0)$ is real analytic (see Refs. 13), hence $\mathcal{F}(E+i\epsilon, 0) = \mathcal{F}^*(E+i\epsilon,0)$, and the discontinuity of $\mathcal{F}$ across the unitarity cuts involves only $\mathrm{Im}\mathcal{F}$.

[15]H. Pi (unpublished).

[16]W. Gilbert, Phys. Rev. **108**, 1078 (1957).

[17]M. M. Block and R. N. Cahn, Rev. Mod. Phys. **57**, 563 (1985).

[18]L. Durand and R. Lipes, Phys. Rev. Lett. **20**, 637 (1968).

[19]T. T. Chou and C. N. Yang, Phys. Rev. **170**, 1591 (1968); Phys. Rev. Lett. **20**, 1213 (1968); Phys. Lett. **128B**, 457 (1983).

[20]E. Eichten, I. Hinchliffe, K. Lane, and C. Quigg, Rev. Mod. Phys. **56**, 579 (1984).

[21]The data on σ_{total} and σ_{elastic} in Fig. 1 are from the following references: ISR and lower-energy data, N. Amos *et al.*, Nucl. Phys. **B262**, 689 (1985), and references therein; R. Castaldi and G. Sanguinetti, Annu. Rev. Nucl. Part. Sci. **35**, 351 (1985); UA4 data, M. Bozzo *et al.*, Phys. Lett. **147B**, 392 (1984); UA5 data, G. J. Alner *et al.*, Z. Phys. C **32**, 153 (1986).

[22]The cosmic-ray data on σ_{total} in Fig. 1 are from the following references: Akeno data, T. Hara *et al.*, Phys. Rev. Lett. **50**, 2058 (1983); Fly's Eye data, R. M. Baltrusaitis *et al.*, *ibid.* **52**, 1380 (1984). The Akeno p-air data were converted to pp cross sections using the value $\sigma_{\text{total}}(pp)=120$ mb given for the Fly's Eye point in the second reference, and the scaling curves in G. B. Yodh, Ann. N.Y. Acad. Sci. **461**, 239 (1986).

[23]The data on $\Delta\sigma=\sigma_{\bar{p}p}-\sigma_{pp}$ in Fig. 2 are from N. Amos *et al.* (Ref. 21) and from A. S. Carroll, Phys. Lett. **61B**, 303 (1976).

[24]The data on $d\sigma/dt$ for $\bar{p}p$ scattering at $\sqrt{s}=546$ GeV in Fig. 3 are from M. Bozzo *et al.*, Phys. Lett. **155B**, 197 (1985).

[25]The data on B_{pp} and $B_{\bar{p}p}$ in Fig. 4 are from the following references: ISR and lower-energy data, N. Amos *et al.* (Ref. 21); UA4 data, M. Bozzo *et al.*, Phys. Lett. **147B**, 385 (1984); Tevatron data, N. A. Amos *et al.*, Phys. Rev. Lett. **61**, 525 (1988).

[26]Data on ρ_{pp} and $\rho_{\bar{p}p}$ are from the following references: ISR and lower-energy data, N. Amos *et al.* (Ref. 21); L. A. Fajardo *et al.*, Phys. Rev. D **24**, 461 (1981); UA4 data, D. Bernard *et al.*, Phys. Lett. B **198**, 583 (1987).

[27]T. Stanev, in *Physics Simulations at High Energy* (Ref. 2), pp. 141–152.

[28]G. B. Yodh (Ref. 22); in *Physics Simulations at High Energy* (Ref. 2), pp. 153–165.

[29]L. Durand and H. Pi, Phys. Rev. D **38**, 78 (1988).

[30]M. M. Block, report at the 1989 Aspen Winter Particle Physics Conference (unpublished).

[31]R. J. Glauber and J. Velasco, Phys. Lett. **147B**, 380 (1984).

[32]L. V. Gribov, E. M. Levin, and M. G. Ryskin, Phys. Rep. **100**, 1 (1983); J. Kwieciński, Z. Phys. C **29**, 147 (1985); A. H. Mueller and J. Qiu, Nucl. Phys. **B268**, 427 (1986).

[33]A different derivation of this decomposition based on the Abramovski-Kancheli-Gribov cutting rules of Reggeon field theory or perturbative QCD is given by R. Blankenbecler, A. Capella, J. Tran Thanh Van, C. Pajares, and A. V. Ramallo, Phys. Lett. **107B**, 106 (1981); see also T. K. Gaisser and T. Stanev, Phys. Lett. B **219**, 375 (1989).

[34]B. Humpert, Phys. Lett. **131B**, 461 (1983); N. Paver and D. Treleani, *ibid.* **146B**, 252 (1984).